[22] Linehan WM, Vasselli J, Srinivasan R, Walther MM, Merino M, Choyke P, et al. Genetic basis of cancer of the kidney disease-specific approaches to therapy. Clin Cancer Res 2004;10:6282s–9s.
[23] Klomp JA, Petillo D, Niemi NM, Dykema KJ, Chen J, Yang XJ, et al. Birt-Hogg-Dubé renal tumors are genetically distinct from other renal neoplasias and are associated with up-regulation of mitochondrial gene expression. BMC Med Genet 2010;3:59. http://dx.doi.org/10.1186/1755-8794-3-59.
[24] Pavlovich CP, Grubb RL, Hurley K, Glenn GM, Toro J, Schmidt LS, et al. Evaluation and management of renal tumors in the Birt-Hogg-Dubé syndrome. J Urol 2005;173:1482–6.
[25] Tobino K, Seyama K. Birt-Hogg-Dubé syndrome with renal angiomyolipoma. Intern Med 2012;51:1279–80.
[26] Gupta GN, Peterson J, Daryanani KA, Pinto PA, Linehan WM, Bratslavsky G. Oncologic outcomes of partial nephrectomy for multifocal renal cell carcinoma with tumors greater than 4 cm. J Urol 2010;184:59–63.
[27] Tefekli A, Akkaya AD, Peker K, Gümüş T, Vural M, Cezayirli F, et al. Staged, open, no-ischemia nephron-sparing surgery for bilateral-multiple kidney tumors in a patient with Birt-Hogg-Dubé syndrome. Case Rep Med 2012;2012:639629. http://dx.doi.org/10.1155/2012/639629.
[28] Menko FH, van Steensel MA, Giraud S, Friis-Hansen L, Richard S, Ungari S, et al. Birt-Hogg-Dubé syndrome: diagnosis and management. Lancet Oncol 2009;10:1199–206.
[29] Troung LD, Shen SS. Immunohistochemical diagnosis of renal neoplasm. Arch Pathol Lab Med 2011;135:92–109.
[30] Kuroda N, Tanaka A, Ohe C, Nagashima Y. Recent advances of immunohistochemistry of diagnosis of renal tumors. Pathol Int 2013;63:381–90.
[31] Morrison PJ, Donnelly DE, Atkinson E, Maxwell AP. Advances in the genetics of familial renal cancer. Oncologist 2010;15:532–8.
[32] Cheuk W, Los ES, Chan AK, Chan JK. Atypical epithelial proliferation in acquired renal cystic disease harbor cytogenetic aberrations. Hum Pathol 2002;33:761–5.

Please cite this article as: Kuroda N, et al, Intratumoral peripheral small papillary tufts: a diagnostic clue of renal tumors associated with Birt-Hogg-Dubé syndrome, Ann Diagn Pathol (2014), http://dx.doi.org/10.1016/j.anndiagpath.2014.03.002

JJCO Japanese Journal of Clinical Oncology

*Jpn J Clin Oncol 2013;43(3)233–242*
*doi:10.1093/jjco/hyt006*
Advance Access Publication 6 February 2013

# Transition of Organizational Category on Renal Cancer

**Yoji Nagashima[1,*], Naoto Kuroda[2] and Masahiro Yao[3]**

[1]Department of Molecular Pathology, Yokohama City University Graduate School of Medicine, Yokohama, [2]Division of Diagnostic Pathology, Kochi Red Cross Hospital, Kochi and [3]Department of Urology, Yokohama City University Graduate School of Medicine, Yokohama, Japan

*For reprints and all correspondence: Yoji Nagashima, Department of Molecular Pathology, Yokohama City University Graduate School of Medicine, 3-9 Fukuura, Kanazawa-ku, Yokohama 236-0004, Japan.
E-mail: ynagas@med.yokohama-cu.ac.jp

Received April 9, 2012; accepted January 6, 2013

The incidence of kidney cancer is gradually increasing, with a rate of 2–3% per decade. The kidney develops various kinds of neoplasms, some of which are associated with familial cancer syndromes. Such cases have provided clues to identify the cancer-responsible genes. In 2004, the World Health Organization published a new classification system of renal neoplasms, incorporating recent knowledge obtained in the cytogenetic and molecular biological fields, i.e. genes responsible for each histologic subtype (*von Hippel-Lindau* for clear cell renal cell carcinoma, *c-met* for papillary renal cell carcinoma type 1, etc.). Subsequently, the Japanese classification system in 'the General Rule for Clinicopathological Study of Renal Cell Carcinoma' has been revised as the 4th edition, according to the World Health Organization system. Several novel subtypes have been introduced, i.e. mucinous tubular and spindle cell carcinoma, and Xp11.2/*TFE3* translocation-associated renal cell carcinoma. Even after the publication of the classification, other novel subtypes have emerged, i.e. acquired cystic disease-associated renal cell carcinoma and tubulocystic renal cell carcinoma. Additionally, some of the subtypes seem to form families based on morphological transition, immunohistochemical features and gene expression profile. In future, the classification of renal cell carcinoma should be reorganized on the basis of molecular biological characteristics to establish personalized therapeutic strategies.

*Key words: renal cell carcinoma – molecular biology – histopathologic classification*



## INTRODUCTION

The mortality of kidney cancer accounts for 2.2% of cancer deaths in the world and 2.4% in Japan (1). Although its incidence is not necessarily high, the kidney develops various kinds of neoplasms, some of which are associated with familial cancer syndromes (2). Among them, renal epithelial tumors encompass various malignant and benign tumors. Renal epithelial neoplasms have been considered to originate from terminally differentiated tubular epithelial cells via some cell injury followed by acquisition of stem cell properties. Depending on the specific microanatomical site of origin, each type of renal cell carcinoma (RCC) shows unique morphology and property.

In 2004, the World Health Organization (WHO) published a new classification system of renal neoplasms, incorporating recent knowledge obtained in the cytogenetic and molecular biological fields (3). In Japan, 'General Rules for Clinical and Pathological Studies on Cancers' have been used as the guidelines of pathological reporting of each cancer and for renal cell carcinoma, the 'General Rule for Clinical and Pathological Studies on Renal Cell Carcinoma (RCC)' (4). After the publication of the third edition in 1999, it has not

been revised even though new morphological and molecular biological aspects have been found. In 2010, the Japanese classification system in 'the General Rule for Clinical and Pathological Studies on Renal Cell Carcinoma (RCC)' (4) has been revised as the fourth edition, based on the WHO system of 2004. During the improvement of the classification system, novel histologic types were introduced. The RCC associated with Xp11.2 translocations bears translocation involving the *TFE3* gene, predominantly occurs in younger generations and shows relatively indolent clinical outcomes. Mucinous tubular and spindle cell carcinoma is composed of slender tubules and spindle cell fascicles with a mucinous stroma, occurs predominantly in middle-aged female, and is favorable in prognosis. Renal medullary carcinoma is so far limited in the African population bearing the sickle cell trait (5), and neuroblastoma-associated RCC is secondary malignancy occurring after treatment for neuroblastoma (6). The so-called 'granular cell RCC' previously used has reclassified into chromophobe, papillary RCCs and other kinds of renal neoplasms such as oncocytoma and epithelioid angiomyolipoma. As shown in Table 1, the Japanese classification system of RCC has been revised based on the WHO classification. However, there are several subtypes emerging after the publication of the most current classification, i.e. tubulocystic carcinoma, acquired cystic disease (ACD)-associated RCC, etc. (7). Further understanding of renal neoplasm requires the elucidation of relationships between these subtypes including the newly emerging subtypes thereafter.

This review aims to introduce the recent state of histopathologic classification of the renal neoplasms, especially of RCC with molecular biological features, and to provide

**Table 1.** Alteration in the classification of renal epithelial tumors in the 'General Rules for Clinical and Pathological Studies on Renal CellCarcinoma' with newly emerging subtypes and putative groups

| 3rd edition (1999.12.) | 4th edition (2011.4) | Newly emerging subtypes (modified from ref. 7) | Putative groups of the subtypes |
|---|---|---|---|
| Benign adenoma | | | |
| Papillary/papillotubular adenoma | Clear cell type RCC | Tubulocystic carcinoma | Clear cell RCC group |
| Oncocytoma | Multilocular cystic RCC | ACD-associated RCC | Clear cell RCC |
| Metanephric adenoma | Papillary RCC | Thyroid follicle-like carcinoma | Multilocular cystic RCC |
| | Chromophobe RCC | Clear cell papillary RCC | |
| Malignant RCC | Collecting duct carcinoma of Bellini | Oncocytic papillary RCC | Papillary RCC group |
| Clear cell RCC | Renal medullary carcinoma | Leiomyomatous renal carcinoma | Papillary RCC |
| Granular cell RCC | RCC associated with Xp11.2 translocations/*TFE3* gene fusions | RCC associated with 6p21 translocations/*TFEB* gene fusions | Mucinous tubular and spindle cell carcinoma |
| Chromophobe RCC | RCC associated with neuroblastoma | | Tubulocystic carcinoma |
| Spindle cell carcinoma | Mucinous tubular and spindle cell carcinoma | | ACD-associated RCC |
| Cyst-associated RCC | RCC, unclassified | | |
| RCC derived from the cyst | Papillary adenoma | | Chromophobe RCC/oncocytoma group |
| Cystic RCC | Oncocytoma | | Chromophobe RCC |
| Papillary RCC | | | Oncocytoma |
| Collecting duct carcinoma of Bellini | Appendix | | Hybrid oncocytic/chromophobe tumor |
| | Metanephric adenoma | | |
| Miscellaneous | Dialysis-associated renal tumors | | Collecting duct carcinoma group |
| Diaysis-associated RCC | Spindle cell carcinoma | | Collecting duct carcinoma of Bellini |
| | | | Renal medullary carcinoma |
| | | | Translocation-associated RCC group[a] |
| | | | RCC associated with Xp11.2 translocations/*TFE3* gene fusions |
| | | | RCC associated with 6p21 translocations/*TFEB* gene fusions |

ACD, acquired cystic disease; RCC, renal cell carcinoma.
[a]Possesses intimate relationship with angiomyolipoma and epithelioid angiomyolipoma.

information on the relationship between the subtypes including newly emerging ones.

## CLEAR CELL RCC AND THE *VON HIPPEL-LINDAU* GENE

*Clear cell RCC* is the most common epithelial renal neoplasm, which accounts for 70–80% of RCCs. The tumor predominantly occurs in seventh and eighth decades, and the male to female ratio is 2–3:1. The classical symptomatic trias is hematuria, lumbago and lumbodorsal tumor. Radiologically, the tumor is hypervascular. Grossly, the tumor is generally well demarcated from the renal parenchyma, and characteristically yellowish white in color. Hemorrhage and necrosis are frequent.

Histologically, the clear cell RCC is composed of alveolar architectures of the tumor cells (Fig. 1). Between the tumor cell nests, fine vascular networks are observed. The tumor cells are uniform in size, and possess pyknotic and small-sized nuclei and watery clear cytoplasm. The tumor is considered to be derived from the proximal tubular epithelial cells based on the ultrastructural and immunohistochemical investigations. Immunohistochemically, the tumor cells are positive for CD10, CD15, carbonic anhydrase IX and RCC-marker, which are also positive in the proximal epithelium. Its prognosis is dependent on the pathologic stage, nuclear grades and on the presence or absence of sarcomatoid element (8).

More than half of sporadic clear cell RCC possesses molecular abnormalities of the *von Hippel-Lindau* (*VHL*) tumor suppressor gene (9–12), of which product protein negatively regulates hypoxia-inducible factor (HIF) via ubiquitin-proteasome-mediated degradation (13). Subsequently, HIF and the downstream molecules, vascular endothelial growth factor (VEGF) and platelet-derived growth factor show excessive function in clear cell RCC to cause abnormally enhanced angiogenesis (Fig. 2). Therefore, the suppression of angiogenesis via the VHL-HIF-VEGF pathway is expected to provide a sophisticated therapeutic strategy of clear cell RCC (14). Based on this fact, sorafenib and sunitinib are reported to improve the survival periods comparing those in the cytokine era (15). Simultaneously, HIF enhances the transcription of *GLUT-1*, *erythropoietin* and *CXCR4 chemokine receptor* genes, resulting in the formation of glycogen-rich clear cytoplasm, paraneoplastic polycythemia and increased tumor cell motility, respectively (Fig. 2B). These events can interpret the characteristics of clear cell RCC.

*Multilocular cystic RCC* is composed of tumor cells with clear cytoplasm lining the delicate cystic walls. This subtype is considered as a variant of clear cell RCC based on the

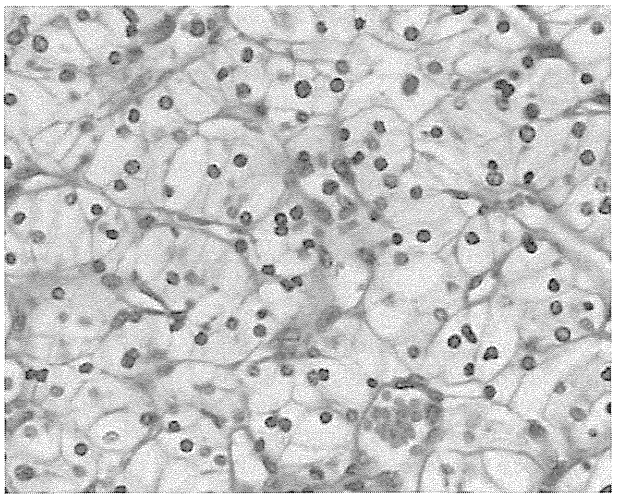

**Figure 1.** Clear cell RCC, representative histology (H&E).

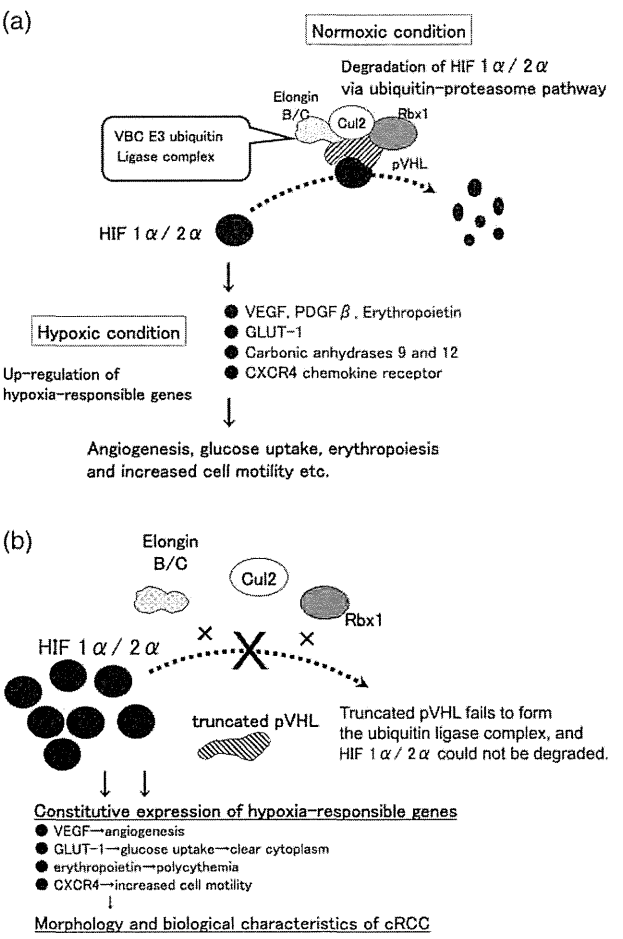


**Figure 2.** The function of pVHL. (a) The physiological function of pVHL. Under a normoxic condition, pVHL forms a ubiquitin ligase complex with elongin B, elongin C, Cul2 and VBP to degrade HIFs 1α and 2α to suppress unnecessary cellular response to hypoxia. Under a hypoxic condition, pVHL and the partners do not degrade the HIFs. HIFs 1α or 2α forms a heterodimeric transcription factor with constitutively expressed HIF1β to induce hypoxic response. (b) In the cases of VHL-mutated RCCs, truncated pVHL failed to form a ubiquitin ligase complex and hypoxic response is constitutively accelerated. Accordingly, abnormal angiogenesis and polycythemia are induced by abnormally expressed VEGF and erythropoietin, respectively.

cellular morphology and frequent *VHL* mutation. Multilocular cystic RCC is distinguished from conventional clear cell RCC, because of its indolent behavior and excellent clinical outcomes (16). Consequently, excessive treatment should be avoided for this subtype, unlike conventional clear cell RCC.

## PAPILLARY RCC AND RELATED SUBTYPES

Papillary RCC is defined as a subtype of RCC, in which papillary architectures is a predominant component. This subtype is considered to relate with newly emerging subtypes, mucinous tubular spindle cell carcinoma, tubulocystic carcinoma and ACD-associated RCC, mainly based on the cDNA expression profiling and immunohistochemistry.

*Papillary RCC* accounts for 7–15% of all the RCC. The age of the patients are similar to clear cell RCC (52–66 years old) and the male to female ratio is 1.8–3.8:1. The initial symptom is also similar to clear cell RCC, and frequently detected with abdominal ultrasonography during health check-up (17).

Grossly, the tumor is well demarcated from the renal parenchyma. The capsule might be thick and firm. The cut surface is golden yellow and muddy. Hemorrhage and necrosis are frequent.

Microscopically, the tumor is predominantly composed of papillary architectures of tumor cells as its definition. The cores contain small blood vessels and fibrous tissue. According to the cellular atypism, papillary RCC is subclassified into two subtypes, that is, type 1 and type 2 (18). Tumor cells of type 1 papillary RCC are small in size, and possess small round nuclei and pale to basophilic cytoplasm (Fig. 3a). The nuclear atypism is mild. Tumor cells are arranged in a monolayered manner. In contrast, tumor cells of type 2 are moderate to large in size, and possess larger nuclei with marked atypism and eosinophilic cytoplasm (Fig. 3b). The tumor cells are arranged in a pseudostratified manner. Type 2 tumor shows more unfavorable clinical outcomes than type 1 (17,18).

Immunohistochemically, the tumor cells are characteristically positive for α-methyl acyl CoA racemase (AMACR) and CD10 (19). Generally, papillary RCC shows the immunophenotypes resembling the proximal tubular epithelial cells. Cytogenetically, trisomy or tetrasomy 7, trisomy 17 and loss of Y chromosome are characteristic to papillary RCC. Additionally, familial type 1 cancer is reported to bear gain-of-function mutation of *c-met* and familial type 2 loss-of-function mutation of *fumarate hydratase* (*FH*) gene (20).

*Mucinous tubular and spindle cell carcinoma* (*MTSCC*) is a newly introduced subtype. MTSCC occurs predominantly in middle aged to elderly females. Most of the cases are detected incidentally. Radiologically, the tumor is well demarcated and hypovascular, without necrosis or hemorrhage.

Grossly, the tumor is well demarcated, and elastic to firm in consistency. The cut surface is milky white and homogenous in color. Hemorrhage and necrosis are absent.

MTSCC is composed of tubular architectures of cuboidal epithelial cells and fascicles of spindle cells. The tumor cells possess small round nuclei and scanty clear cytoplasm (Fig. 3c). Generally, its prognosis is favorable, except for few cases. Because the tumor cells partly possess immunophenotypes similar to those of the distal tubular and collecting ductal epithelial cells, MTSCC is initially referred as low-grade collecting duct carcinoma. However, cDNA profiling indicates an intimate relationship with papillary RCC. Additionally, similar immunophenotypes including positivity with AMACR has been reported (21,22), although different karyotypic abnormalities between them have been also observed (23).

The clinical outcomes are generally favorable. Consequently, pathological diagnosis should be precise to avoid excessive treatment. However, there are several case reports of aggressive cases of MTSCC (24).

In patients with long-term hemodialysis, the morbidity of RCC increases from 5- to 6-folds, comparing with non-dialysis patients. The ages of initial diagnosis are younger by 5–10 years, comparing with non-dialysis group. The male-to-female ratio is 5–6:1. Characteristically, the kidneys present marked parenchymal atrophy with multiple cysts, the so-called ACD of the kidney. Together with the unusual histology, dialysis-associated RCC is considered to possess a unique carcinogenic mechanism and clinicopathological characteristics to be clarified (25). Tickoo et al. (26) reviewed 261 tumors occurring in end-stage renal disease cases. They reported that approximately half of the cases examined could be classified into the subtypes listed in the WHO classification. The rest of the cases were classified into two groups: (1) *ACD-associated RCC* composed of solid and microcystic architectures of granular tumor cells (Fig. 3d) and (2) clear cell-papillary RCCs (not described in this review). At least, ACD-associated RCC seems to bear chromosomal abnormalities different from the other RCC subtypes (27). Several gene profile studies on ACD-associated RCC revealed features similar to papillary RCC, as well as morphologic transition and immunohistochemical similarities (AMACR and CK7).

*Tubulocystic RCC*, a new subtype not included in the recent classification, forms a well-circumscribed mass composed of pure tubular and cystic architectures. The wall of the tubules and cysts are lined with tall columnar epithelial cells (Fig. 3e). Their nuclei are large with prominent nucleoli and the cytoplasm is eosinophilic and granular (28). Immunohistochemically, the tumor cells are positive for AMACR and CK7, like papillary RCC. Originally, this subtype had been recognized as low-grade collecting duct carcinoma as presented in the atlas published by the Armed Forces Institute of Pathology (29). Generally, this subtype usually occurs in patients older than 60 years (34–94 years old) with a strong male predominance (7:1).

Described as above, the papillary RCC is a prototype of a larger family of subtypes. Actually, composite tumors are reported, which possess a papillary RCC element with

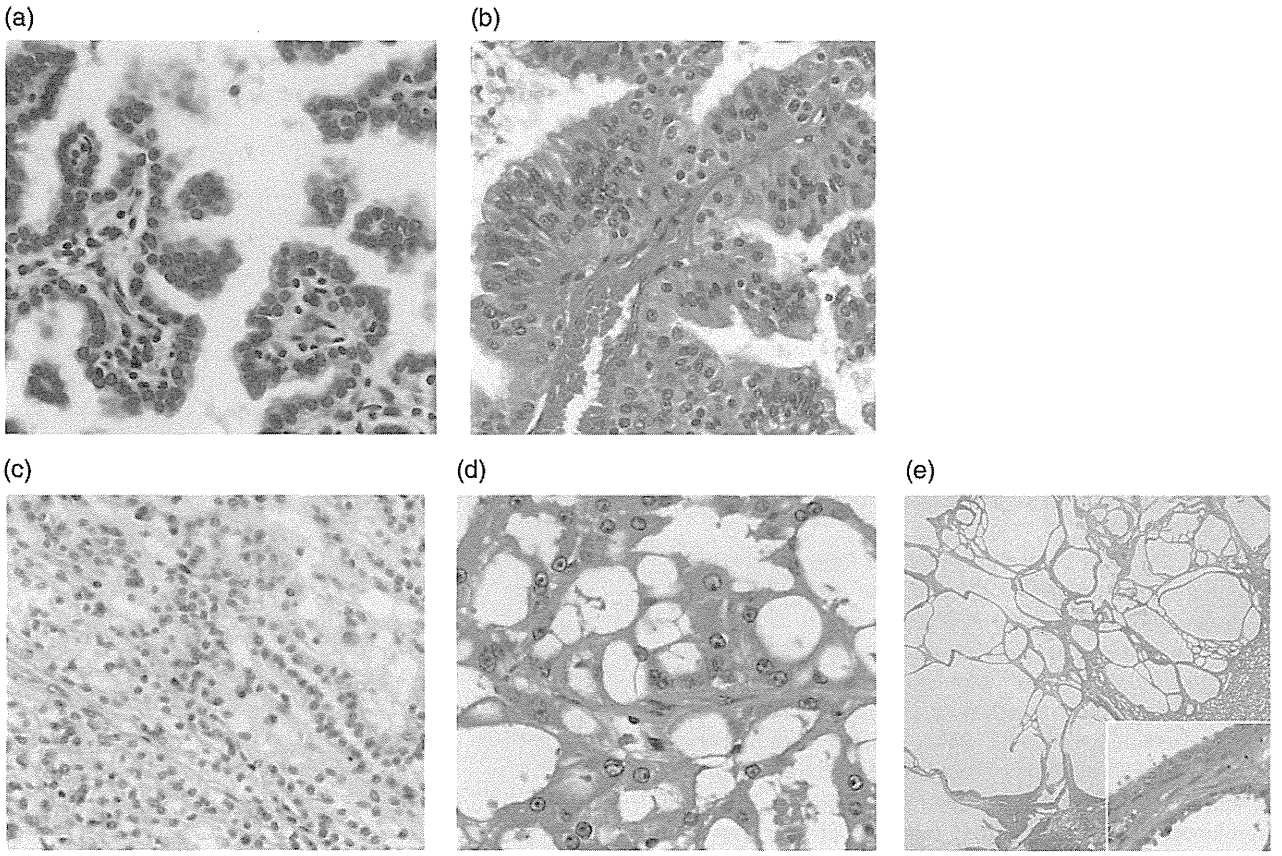


**Figure 3.** Papillary RCC type 1 (a) and type 2 (b), and of probably relating subtypes (c–e), representative histology. (c) Mucinous tubular and spindle cell carcinoma. (d) ACD-associated RCC. (e) Tubulocystic RCC. The tumor is composed of various-sized cysts lined with tumor cells (H&E).

gradual transition to mucinous tubular and spindle cell carcinoma as well as to tubulocystic carcinoma. ACD-associated RCC has been diagnosed as 'papillary RCC', but frequently histological transition to papillary RCC is noted.

## CHROMOPHOBE RCC AND ONCOCYTOMA

*Chromophobe RCC* accounts for ~5–10% of RCC, and characteristically possesses cloudy and reticular cytoplasm. Since the first report in human by Thoenes et al. (30), investigators have clarified different characteristics of chromophobe RCC from the clear cell RCC.

The chromophobe RCC occurs in somewhat younger generation, comparing with clear cell RCC. Male and female are equally involved. Clinical presentation is mainly renal tumor detected with ultrasonography on routine health check-up. However, abdominal palpable tumor might be an initial presentation, because of its huge size.

Grossly, the tumor is generally well demarcated from the surrounding parenchyma, and forms a large homogenous mass with beige color. Necrosis or hemorrhage is scarce.

Histologically, the tumor is composed of solid cell sheets, trabecular and glandular architectures of the tumor cells. The tumor cells are large in size and polygonal in shape. The cytoplasmic rims are accentuated to give a 'plant cell-like' appearance. The nuclei are irregular in configuration, which are frequently referred as 'raisin like (rasinoid)'. Characteristically, the cytoplasm is weakly eosinophilic and cloudy or reticular (typical variant). Occasionally, tumor cells with eosinophilic granular cytoplasm (eosinophilic variant) might be intermingled. Eosinophilic variant frequently gives difficulties in differential diagnosis between oncocytoma. Although the nuclei are scored as high grade in atypism, chromophobe RCC possesses a more favorable prognosis than clear RCC (31) (Fig. 4a). However, chromophobe RCC is known to develop a sarcomatoid change in a higher frequency than the other subtypes (32,33). The tumor cells are diffusely positive for colloid iron staining. Ultrastructurally, the cytoplasm is filled with numerous microvesicles probably derived from mitochondrial membrane. In eosinophilic variant, mitochondria are more abundant.

Immunohistochemically, the tumor cells are positive for epithelial membrane antigen (EMA), E-cadherin (34) and c-KIT (35,36). These markers are positive in those of the distal tubular and collecting ductal epithelial cells, which are the origin of chromophobe RCC.

Chromophobe RCC shows non-random multiple chromosome loss (37). The gene responsible for chromophobe RCC is not identified. The *FCLN* gene, responsible for Birt-Hogg-Dubé syndrome, is a candidate (described later) (38). Several studies have been performed on the alteration of the *FCLN* gene in renal neoplasms, but the results are not consistent (39).

*Oncocytoma* is a benign neoplasm of the kidney, which is composed of solid cell sheets of uniform and round tumor cells. The cytoplasm is characteristically eosinophilic and granular.

The patients of oncocytoma show a peak in the seventh decade. The gender deviation has not been described. Most of the cases are incidentally found during abdominal ultrasonography during health check-up. Radiologically, the tumor presents a spoke-wheel like vasculature on angiography. All the cases are successfully treated by radical or partial nephrectomy.

Grossly, the tumor is well demarcated from the renal parenchyma without capsule formation. The cut surface is mahogany in color with a frequent central scar.

Microscopically, the tumor is composed of cell nests with an edematous stroma. The tumor cells are uniform and small in size. Notably, their cytoplasm is characteristically eosinophilic and granular (Fig. 4b), which coincide with numerous mitochondria. The immunohistochemical characteristics of the tumor cells show positivities for E-cadherin, c-kit and mitochondrial antigen, similar to those of chromophobe RCC (reviewed in ref. 40)

Because of various similar features, differential diagnosis between chromophobe RCC and oncocytoma is frequently challenging. The pathobiological features shared by these tumors (13) are as follows: (i) morphological similarities, i.e. eosinophilic and granular cytoplasm, (ii) mitochondrial abnormalities are suggested, i.e. vesicles probably derived from the mitochondria in chromophobe RCC and numerous mitochondria present in oncocytoma, (iii) similar lectin histochemical and immunohistochemical results (34) and (iv) mitochondrial DNA alteration reported by some investigators (41). To make a differential diagnosis of these two, the notable points were listed in Table 2.

Recent reports demonstrated the existence of hybrid tumor containing elements of chromophobe RCC and oncocytoma (42). Furthermore, both tumors develop in BHD syndrome, an autosomal dominant-inherited familial tumor syndrome, which shows fibrofolliculoma of the head and neck, spontaneous pneumothorax caused by the rupture of pneumatocele and multiple renal tumors (43). The responsible gene, *Folliculin*, *FLCN* is a tumor-suppressor gene located in chromosome 17p11.2, encoding a protein named as folliculin (38). Although the exact roles of folliculin in renal carcinogenesis remains to be elucidated, recent studies revealed that folliculin is involved in AMPK and mTOR signaling pathways, and that artificial Flcn inactivation in the murine kidney generates severe polycystic changes in the kidney (44,45). Considering these facts, *FCLN* mutation in this case caused abnormal cell growth in the kidney resulting in renal epithelial tumors. Consequently, the *FLCN* gene is expected to play some role in the development of chromophobe RCC and oncocytoma (46).

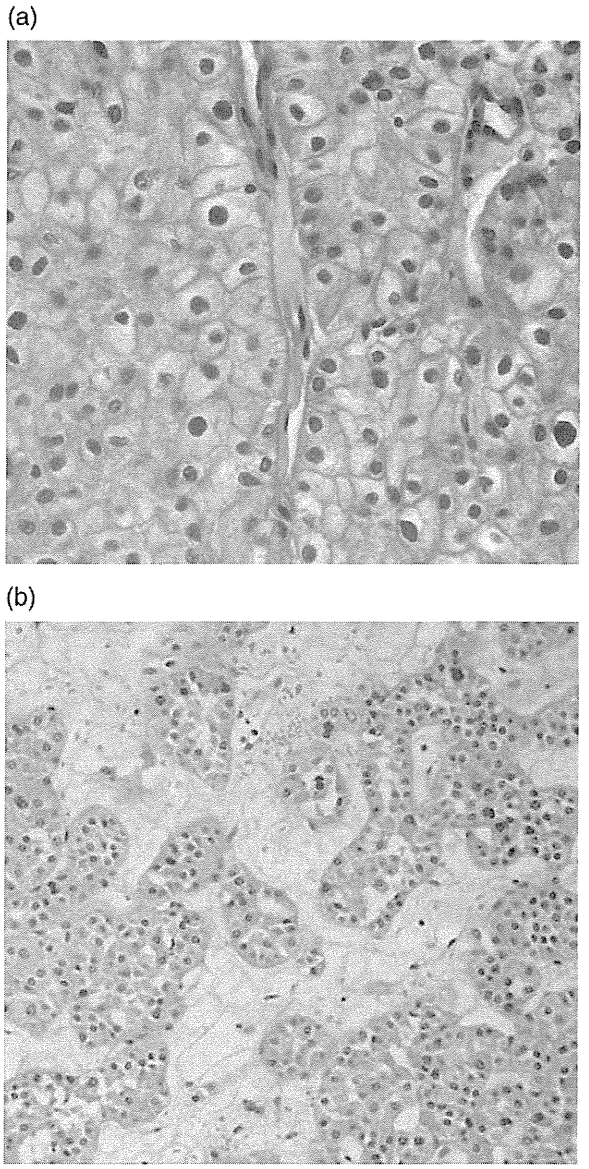


**Figure 4.** Chromophobe RCC and oncocytoma. (a) Chromophobe RCC, representative histology. (b) Oncocytoma, representative histology (H&E).

## TRANSLOCATION-ASSOCIATED RCCS

Recently, RCCs occurring in the childhood and young generation are known to bear characteristic chromosomal translocations involving *transcription factor enhancer* genes, *TFE3* on Xp11.2 and *TFEB* on 6p21.

The *Xp11.2/TFE3 translocation-associated RCCs* are mostly composed of papillary or nested patterns of the tumor

**Table 2.** Differential diagnosis between chromophobe RCC and oncocytoma (ref. 3,31,34)

| | Chromophobe RCC | Oncocytoma |
|---|---|---|
| Gross findings | Beige, homogenous | Mahogany, central scar |
| Microscopic findings | | |
| Architecture | Solid sheet-like, tubular, cystic | Alveolar, organoid, solid, tubular |
| Nuclei | Cleaved, rasinoid | Round |
| Cell boundary | Definite | Obscure |
| Stroma | Hypovascular | Edematous or hyalinized |
| Colloidal iron stain | Diffusely positive | Negative or positive limited to the apical surface |
| Immunohistochemistry | | |
| CD82 | Positive | Negative |
| CK7 | Diffusely positive | Focally positive or negative |
| S100A1 | Negative | Positive |
| Electron microscopy | Numerous microvesicles | Abundant mitochondria |
| Cytogenetics | Multiple chromosome loss | Normal; deletion #1 and/or #14; translocation involving #11q12–13 |

#, chromosome.

cells with clear and weakly eosinophilic cytoplasm. The nuclear atypism is higher than conventional clear cell RCC. Microcalcification and psammoma bodies are frequent (Fig. 5a). Radiologically, these tumors are hypovascular. Their prognoses are reported to be mostly indolent even though their clinical stage might be advanced. However, it could be aggressive, especially when occurring in elderly patients (47).

Although this kind of tumors has been diagnosed as clear cell RCC or papillary RCC (see bellows), Argani et al. (48) reported that these tumors bear chromosomal translocation involving #Xp11.2 and several kinds of partners (Table 3). As the results of translocation, *TFE3* fuses with *ASPS/PRCC17*, *PMF* and *CLTC*. In cases of inversion, a fusion gene, *TFE3-NonO* is generated. *TFE3-ASPS/PRCC17* is also formed in the alveolar soft part sarcoma, a malignancy occurring in the limb skeletal muscle of the young generation (49). Whatever the partner gene is, the fusion gene product (chimeric protein) has a sustained turnover than the native TFE3 protein. Subsequently, immunohistochemical staining for TFE3 shows nuclear staining in the translocation RCCs, which is a diagnostic hallmark of *TFE3*-translocation RCCs as well as in alveolar soft part sarcoma (50).

On the other hand, RCC with *t(6;11)(p21.1;q12)* chromosome translocation generates the *TFEB* (transcription factor enhancer B)—$\alpha$ fusion gene (51,52). TFE3 and TFEB form a transcription factor family together with the microphthalmia transcription factor (MiTF) and TFEC, called the MiTF/TFE transcription factor family. Therefore, these translocation-associated RCCs seem to have an intimate relationship with each other (53). This subtype is composed of papillary or solid architectures surrounding the basement membrane-like matrix in the center. The tumor cells show the so-called biphasic morphology, that is, larger and smaller ones. The larger cells possess large vesicular nuclei and voluminous clear cytoplasm and the smaller cells small round nuclei and scanty cytoplasm similar to that of lymphocytes (Fig. 5b).

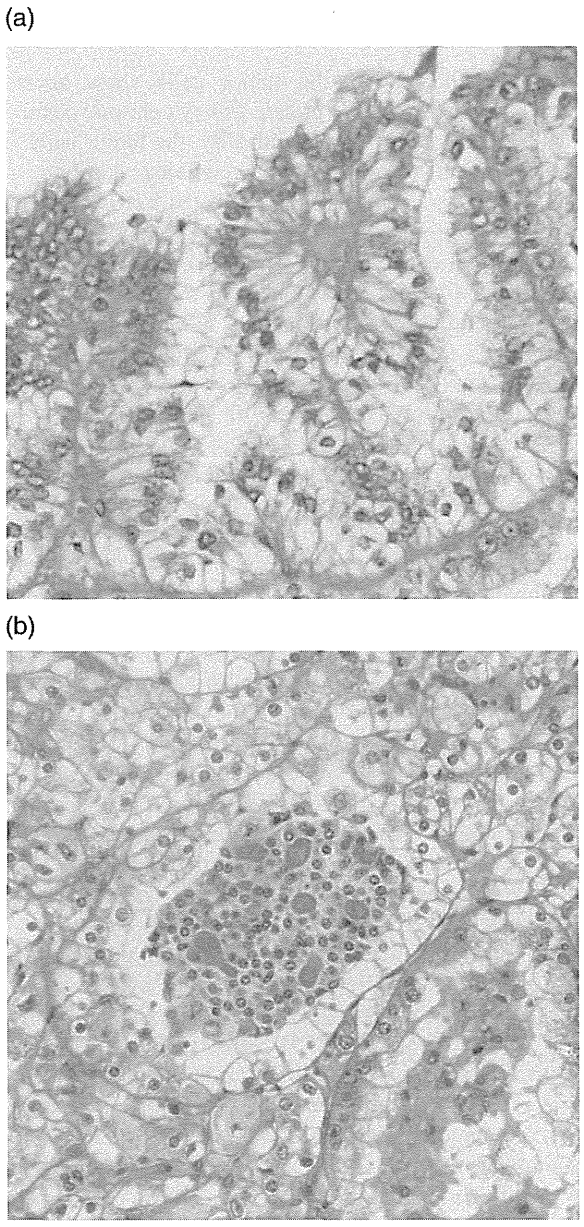


**Figure 5.** Translocation-associated RCCs. (a) RCC associated with Xp11.2 translocations/*TFE3* gene fusions, representative histology and (b) 6p21/*TFEB* translocation-associated RCC. Note the microcystic structure containing smaller cells with matrix substance.

**Table 3.** Translocations identified in Xp11.2/*TFE3*- and 6p21/*TFEB*-translocation-associated RCCs (ref. 47–52)

| Translocation | Resultant fusion genes |
|---|---|
| t(X;17)(p11.2;q21.2) | *PRCC-TFE3* |
| t(X;1)(p11.2;p34) | *PSF-TFE3* |
| t(X;17)(p11.2;q25.3) | *ASPL/RCC17-TFE3* |
| t(X;17)(p11.2;q23) | *CLTC-TFE3* |
| inv(X)(p11.2;q12) | *NonO-TFE3* |
| t(6;11)(p21:q13) | *TFEB-α* |

Immunohistochemically, the tumor cells show aberrant nuclear positivity for TFEB protein and cytoplasmic positivity for cathepsin K (54). Characteristically, the tumor cells frequently present positivity for melanoma markers, i.e. melanosome-associated antigen (detected by HMB45 antibody), but negativity for epithelial markers, i.e. cytokeratin and epithelial membrane antigen (55,56). Although its prognosis is generally indolent, more cases should be evaluated before a conclusion is established.

Both TFE3 and TFEB belong to a transcription family, MiTF/TFE family. MiTF is the master regulator of melanocyte differentiation. Together with the positive reaction with HMB45 (an antibody raised against a melanosome-associated antigen) and positivities of melanocyte markers (Melan A, tyrosinase, MiTF), the translocation-associated RCCs seem to possess some relationship with melanoma. Furthermore, melanotic cases have been reported.

On the other hand, angiomyolipoma and epithelioid angiomyolipoma are non-epithelial tumors, which are frequently associated with tuberous sclerosis (TSC) and bears the aberrations of TSC-responsible genes, *TSC-2* and *TSC-1*. They are known to be positive for melanocyte markers. Whereas the former is composed of dysmorphic thick-walled blood vessels, leiomyomatous spindle cells and mature fat, the latter purely composed of highly atypical polygonal cells with epithelioid arrangements, mimicking carcinoma. Therefore, some of epithelioid angiomyolipoma is considered to be misdiagnosed as high-grade RCC, before the establishment of epithelioid angiomyolipoma by Eble et al. (53). Both conventional and epithelioid angiomyolipoma show immunoreactivities with melanocyte markers, i.e. melanosome-associated antigen detected by HMB45, MiTF, Melan A and tyrosinase (55). Interestingly, TFE3- and TFEB-translocation-associated RCCs are composed of polygonal cells with an epithelioid arrangement, which mimic epithelioid angiomyolipoma. Translocation-associated RCCs occasionally show melanin production and deposition as well as epithelioid angiomyolipoma. Together with the morphological findings and similar immunohistochemical natures, epithelioid angiomyolipoma and translocation-associated RCCs might form a disease family, which should be evaluated in future.

## CONCLUSION

Recent advances in molecular biology have altered the classification of renal epithelial tumors. Especially, excessive function of HIF-VEGF pathway provides a molecular target therapy for clear cell RCC. For other subtypes, tailored medicine will be established.

Whether all the tumors with a specific gene abnormality show same morphology should be elucidated in future. If the common pathway is involved, different kinds of tumors could develop. For example, abnormalities both of *TSC2* and of *FCLN* are expected to cause excessive function of the mTOR pathway. However, the former causes angiomyolipoma and epithelioid angiomyolipoma, whereas the latter causes chromophobe RCC, oncocytoma and hybrid chromophobe/oncocytic tumor.

Finally, tumors with low-grade malignancy have emerged (mucinous tubular and spindle cell carcinoma, ACD-associated RCC, tubulocystic RCC), for which excessive treatment should be avoided. For renal epithelial tumors, precise histological diagnosis is required based on the molecular biological knowledge to establish individualized therapeutic strategies.

## Acknowledgements

The authors acknowledge Ms Tamiyo Taniguchi and Sayuri Kanaya for their assistance.

## Funding

Our original works cited in this review were supported by grants-in-aid from the Japanese Ministry of Education, Culture, Sports and Science and from the Yokohama Foundation for Promotion of Medicine.

## Conflict of interest statement

None declared.

## References

1. GLOBOCAN 2008. http://globocan.iarc.fr/ (12 March 2012, date last accessed).
2. Nagashima Y, Kobayashi N, Kagawa E, Aoki I, Inayama Y, Yao M. Pathology and molecular biology of renal neoplasms. Recent advances and impacts on pathological classification. In: Nakamura M, Kakudo K, editors. *Molecular Mechanism and Morphology in Cancer*. Oak Park, IL: Bentham Science Publishers E-Book 2009;12–41.
3. Eble JN, Sauter G, Epstein JI, Sesterhenn IA. Chapter 1: Tumours of the kidney. In: Eble JN, Sauter G, Epstein JI, Sesterhenn IA, editors. *World Health Organization Classification of Tumours. Pathology & Genetics Tumours of the Urinary System and Male Genital Organs*. Lyon: IARC Press 2004;9–43.
4. Japanese Urological Association, Japanese Society of Pathology, Japan Radiological Society. *General Rules for Clinical and Pathological*

*Studies on Renal Cell Carcinoma*. 4th edn. Tokyo, Japan: Kanehara Shuppan 2011 (in Japanese).
5. Gupta R, Billis A, Shah RB, et al. Carcinoma of the collecting ducts of Bellini and renal medullary carcinoma: clinicopathologic analysis of 52 cases of rare aggressive subtypes of renal cell carcinoma with a focus on their interrelationship. *Am J Surg Pathol* 2012;36:1265–78.
6. Medeiros LJ, Palmedo G, Krigman HR, Kovacs G, Beckwith JB. Oncocytoid renal cell carcinoma after neuroblastoma: a report of four cases of a distinct clinicopathologic entity. *Am J Surg Pathol* 1999;23:772–80.
7. Srigley JR, Delahunt B. Uncommon and recently described renal carcinomas. *Mod Pathol* 2009;22:S2–S23.
8. Amin MB, Amin MB, Tamboli P, et al. Prognostic impact of histologic subtyping of adult renal epithelial neoplasms: an experience of 405 cases. *Am J Surg Pathol* 2002;26:281–91.
9. Shuin T, Kondo K, Torigoe S, et al. Frequent somatic mutations and loss of heterozygosity of the von Hippel-Lindau tumor suppressor gene in primary human renal cell carcinomas. *Cancer Res* 1994;54:2852–5.
10. Kondo K, Yao M, Yoshida M, et al. Comprehensive mutational analysis of the VHL gene in sporadic renal cell carcinoma: relationship to clinicopathological parameters. *Genes Chromosomes Cancer* 2002;34:58–68.
11. Kim WY, Kaelin WG. Role of VHL gene mutation in human cancer. *J Clin Oncol* 2004;22:4991–5004.
12. Gossage L, Eisen T. Alterations in VHL as potential biomarkers in renal-cell carcinoma. *Nat Rev Clin Oncol* 2010;7:277–88.
13. Maxwell PH, Wiesener MS, Chang GW, et al. The tumour suppressor protein VHL targets hypoxia-inducible factors for oxygen-dependent proteolysis. *Nature* 1999;399:271–5.
14. Ahmed Z, Bicknell R. Angiogenic signalling pathways. *Methods Mol Biol* 2009;467:3–24.
15. Singer EA, Gupta GN, Srinivasan R. Targeted therapeutic strategies for the management of renal cell carcinoma. *Curr Opin Oncol* 2012;24:284–90.
16. Kuroda N, Ohe C, Mikami S, et al. Multilocular cystic renal cell carcinoma with focus on clinical and pathobiological aspects. *Histol Histopathol* 2012;27:969–74.
17. Kuroda N, Toi M, Hiroi M, Enzan H. Review of papillary renal cell carcinoma with focus on clinical and pathobiological aspects. *Histol Histopathol* 2003;18:487–94.
18. Delahunt B, Eble JN. Papillary renal cell carcinoma: a clinicopathologic and immunohistochemical study of 105 tumors. *Mod Pathol* 1997;10:537–44.
19. Tretiakova MS, Sahoo S, Takahashi M, et al. Expression of alpha-methylacyl-CoA racemase in papillary renal cell carcinoma. *Am J Surg Pathol* 2004;28:69–76.
20. Alam NA, Rowan AJ, Wortham NC, et al. Genetic and functional analyses of FH mutations in multiple cutaneous and uterine leiomyomatosis, hereditary leiomyomatosis and renal cancer, and fumarate hydratase deficiency. *Hum Mol Genet* 2003;12:1241–52.
21. Paner GP, Srigley JR, Radhakrishnan A, et al. Immunohistochemical analysis of mucinous tubular and spindle cell carcinoma and papillary renal cell carcinoma of the kidney: significant immunophenotypic overlap warrants diagnostic caution. *Am J Surg Pathol* 2006;30:13–9.
22. Shen SS, Ro JY, Tamboli P, et al. Mucinous tubular and spindle cell carcinoma of kidney is probably a variant of papillary renal cell carcinoma with spindle cell features. *Ann Diagn Pathol* 2007;11:13–21.
23. Cossu-Rocca P, Eble JN, Delahunt B, et al. Renal mucinous tubular and spindle carcinoma lacks the gains of chromosomes 7 and 17 and losses of chromosome Y that are prevalent in papillary renal cell carcinoma. *Mod Pathol* 2006;19:488–93.
24. Bulimbasic S, Ljubanovic D, Sima R, et al. Aggressive high-grade mucinous tubular and spindle cell carcinoma. *Hum Pathol* 2009;40:906–7.
25. Ishikawa I, Kovacs G. High incidence of papillary renal cell tumours in patients on chronic haemodialysis. *Histopathology* 1993;22:135–9.
26. Tickoo SK, de Peralta-Venturina MN, Harik LR, et al. Spectrum of epithelial neoplasms in end-stage renal disease: an experience from 66 tumor-bearing kidneys with emphasis on histologic patterns distinct from those in sporadic adult renal neoplasia. *Am J Surg Pathol* 2006;30:141–53.
27. Cossu-Rocca P, Eble JN, Zhang S, Martignoni G, Brunelli M, Cheng L. Acquired cystic disease-associated renal tumors: an immunohistochemical and fluorescence in situ hybridization study. *Mod Pathol* 2006;19:780–7.
28. Yang XJ, Zhou M, Hes O, et al. Tubulocystic carcinoma of the kidney: clinicopathologic and molecular characterization. *Am J Surg Pathol* 2008;32:177–87.
29. Murphy WM, Grignon DJ, Perlman EJ, editors. Tumors of the Kidney, Bladder, and Related Urinary Structures. AFIP Atlas of Tumor Pathology Series 4, Fascicle 1. Silver Spring, MA: ARP Press 2004.
30. Thoenes W, Störkel S, Rumpelt HJ. Human chromophobe cell renal carcinoma. *Virchows Arch B* 1985;48:207–17.
31. Nagashima Y. Chromophobe renal cell carcinoma: clinical, pathological and molecular biological aspects. *Pathol Int* 2000;50:872–8.
32. Akhtar M, Tulbah A, Kardar AH, Ali MA. Sarcomatoid renal cell carcinoma: the chromophobe connection. *Am J Surg Pathol* 1997;21:1188–95.
33. Nagashima Y, Okudela K, Osawa A, et al. Chromophobe renal cell carcinoma with sarcomatoid change. A case report. *Pathol Res Pract* 2000;196:647–51.
34. Taki A, Nakatani Y, Misugi K, Yao M, Nagashima Y. Chromophobe renal cell carcinoma: an immunohistochemical study of 21 Japanese cases. *Mod Pathol* 1999;12:310–17.
35. Yamazaki K, Sakamoto M, Ohta T, Kanai Y, Ohki M, Hirohashi S. Overexpression of KIT in chromophobe renal cell carcinoma. *Oncogene* 2003;22:847–52.
36. Petit A, Castillo M, Mellado B, Mallofre C. c-kit overexpression in chromophobe renal cell carcinoma is not associated with c-kit mutation of exons 9 and 11. *Am J Surg Pathol* 2005;29:1544–45.
37. Shuin T, Kondo K, Sakai N, et al. A case of chromophobe renal cell carcinoma associated with low chromosome number and microsatellite instability. *Cancer Genet Cytogenet* 1996;86:69–71.
38. Nickerson ML, Warren MB, Toro JR, et al. Mutations in a novel gene lead to kidney tumors, lung wall defects, and benign tumors of the hair follicle in patients with the Birt-Hogg-Dubé syndrome. *Cancer Cell* 2002;2:157–64.
39. Gad S, Lefèvre SH, Khoo SK, et al. Mutations in BHD and TP53 genes, but not in HNF1beta gene, in a large series of sporadic chromophobe renal cell carcinoma. *Br J Cancer* 2007;96:336–40.
40. Kuroda N, Toi M, Hiroi M, Shuin T, Enzan H. Review of renal oncocytoma with focus on clinical and pathobiological aspects. *Histol Histopathol* 2003;18:935–42.
41. Kovacs A, Storkel S, Thoenes W, Kovacs G. Mitochondrial and chromosomal DNA alterations in human chromophobe renal cell carcinomas. *J Pathol* 1992;167:273–7.
42. Mai KT, Dhamanaskar P, Belanger E, Stinson WA. Hybrid chromophobe renal cell neoplasm. *Pathol Res Pract* 2005;201:385–9.
43. Schmidt LS, Warren MB, Nickerson ML, et al. Birt-Hogg-Dubé syndrome, a genodermatosis associated with spontaneous pneumothorax and kidney neoplasia, maps to chromosome 17p11.2. *Am J Hum Genet* 2001;69:876–82.
44. Baba M, Furihata M, Hong SB, et al. Kidney-targeted Birt-Hogg-Dubé gene inactivation in a mouse model: Erk1/2 and Akt-mTOR activation, cell hyperproliferation, and polycystic kidneys. *J Natl Cancer Inst* 2008;100:140–54.
45. Hasumi Y, Baba M, Ajima R, et al. Homozygous loss of BHD causes early embryonic lethality and kidney tumor development with activation of mTORC1 and mTORC2. *Proc Natl Acad Sci USA* 2009;106:18722–7.
46. Hudon V, Sabourin S, Dydensborg AB, et al. Renal tumour suppressor function of the Birt-Hogg-Dubé syndrome gene product folliculin. *J Med Genet* 2010;47:182–9.
47. Argani P, Olgac S, Tickoo SK, et al. Xp11 translocation renal cell carcinoma in adults: expanded clinical, pathologic, and genetic spectrum. *Am J Surg Pathol* 2007;31:1149–60.
48. Argani P, Antonescu CR, Illei PB, et al. Primary renal neoplasms with the ASPL-TFE3 gene fusion of alveolar soft part sarcoma: a distinctive tumor entity previously included among renal cell carcinomas of children and adolescents. *Am J Pathol* 2001;159:179–92.
49. Bruder E, Passera O, Harms D, et al. Morphologic and molecular characterization of renal cell carcinoma in children and young adults. *Am J Surg Pathol* 2004;28:1117–32.
50. Argani P, Lal P, Hutchinson B, Lui MY, Reuter VE, Ladanyi M. Aberrant nuclear immunoreactivity for TFE3 in neoplasms with TFE3

gene fusions: a sensitive and specific immunohistochemical assay. *Am J Surg Pathol* 2003;27:750–61.
51. Davis IJ, Hsi BL, Arroyo JD, et al. Cloning of an Alpha-TFEB fusion in renal tumors harboring the t(6;11)(p21;q13) chromosome translocation. *Proc Natl Acad Sci USA* 2003;100:6051–6.
52. Argani P, Hawkins A, Griffin CA, et al. A distinctive pediatric renal neoplasm characterized by epithelioid morphology, basement membrane production, focal HMB45 immunoreactivity, and t(6;11)(p21.1;q12) chromosome translocation. *Am J Pathol* 2001;158:2089–96.
53. Eble JN, Amin MB, Young RH. Epithelioid angiomyolipoma of the kidney: a report of five cases with a prominent and diagnostically confusing epithelioid smooth muscle component. *Am J Surg Pathol* 1997;21:1123–30.
54. Martignoni G, Gobbo S, Camparo P, et al. Differential expression of cathepsin K in neoplasms harboring TFE3 gene fusions. *Mod Pathol* 2011;24:1313–9.
55. Kato I, Inayama Y, Yamanaka S, et al. Epithelioid angiomyolipoma of the kidney. *Pathol Int* 2009;59:38–43.
56. Argani P, Aulmann S, Karanjawala Z, Fraser RB, Ladanyi M, Rodriguez MM. Melanotic Xp11 translocation renal cancers: a distinctive neoplasm with overlapping features of PEComa, carcinoma, and melanoma. *Am J Surg Pathol* 2009;33:609–19.

Epigenetics 8:3, 252–267; March 2013; © 2013 Landes Bioscience

# DNA methylation profiling distinguishes histological subtypes of renal cell carcinoma

Amy A. Slater,[1] Majed Alokail,[1,2] Dean Gentle,[1] Masahiro Yao,[3] Gyula Kovacs,[4] Eamonn R. Maher[1] and Farida Latif[1,*]

[1]Centre for Rare Diseases and Personalised Medicine; Department of Medical & Molecular Genetics; School of Clinical and Experimental Medicine; University of Birmingham College of Medical and Dental Sciences; Birmingham, UK; [2]Department of Biochemistry; Biomarker Research Program; College of Science; King Saud University; Riyadh, Saudi Arabia; [3]Department of Urology; Yokohama City University School of Medicine; Yokohama, Japan; [4]Department of Laboratory Medicine; University of Pecs Medical School; Pecs, Hungary

**Keywords:** renal cell carcinoma, renal oncocytoma, chromophobe renal cell carcinoma, hypermethylation, hypomethylation

Renal cell carcinoma (RCC) accounts for around 3% of cancers in the UK, and both incidence and mortality are increasing with the aging population. RCC can be divided into several subtypes: conventional RCC (the most common, comprising 75% of all cases), papillary RCC (15%) and chromophobe RCC (5%). Renal oncocytoma is a benign tumor and accounts for 5% of RCC. Cancer and epigenetics are closely associated, with DNA hypermethylation being widely accepted as a feature of many cancers. In this study the DNA methylation profiles of chromophobe RCC and renal oncocytomas were investigated by utilizing the Infinium HumanMethylation450 BeadChips. Cancer-specific hypermethylation was identified in 9.4% and 5.2% of loci in chromophobe RCC and renal oncocytoma samples, respectively, while the majority of the genome was hypomethylated. Thirty (hypermethylated) and 41 (hypomethylated) genes were identified as differentially methylated between chromophobe RCC and renal oncocytomas ($p < 0.05$). Pathway analysis identified some of the differentially hypermethylated genes to be involved in Wnt (*EN2*), MAPK (*CACNG7*) and TGFβ (*AMH*) signaling, Hippo pathway (*NPHP4*), and cell death and apoptosis (*SPG20, NKX6-2, PAX3* and *BAG2*). In addition, we analyzed ccRCC and papillary RCC data available from The Cancer Genome Atlas portal to identify differentially methylated loci in chromophobe RCC and renal oncocytoma in relation to the other histological subtypes, providing insight into the pathology of RCC subtypes and classification of renal tumors.

## Introduction

Renal cell carcinomas (RCCs) arise from the epithelium of renal tubules and are the most common type of renal cancers in adults. RCC consists of a group of heterogeneous tumors ranging in their malignant potential from benign to highly tumorigenic. RCCs are classified into four main types: conventional (clear cell), papillary, chromophobe and collecting duct carcinoma. The most common types among these are conventional and papillary, which together account for 85–90% of all RCCs. Chromophobe RCC accounts for 5% of renal tumors and is histologically similar to renal oncocytoma, a benign kidney neoplasm, accounting for another 5% of renal tumors.[1] Each histological subtype harbors different genetic, biological and clinical properties and responds differently to therapy.

Although the vast majority of renal tumors occur sporadically, several inherited cancer syndromes are associated with the development of renal cancer.[2,3] These include von Hippel-Lindau syndrome, hereditary papillary RCC, hereditary leiomyomatosis and Birt-Hogg-Dube syndrome (BHD). Much of our knowledge base for the molecular basis of sporadic RCC has been achieved by identification and functional characterization of the genes predisposing to the familial RCCs mentioned above (*VHL, MET, FH* and *FLCN*, respectively).[4-7] Second generation sequencing projects have led to the identification of additional genes implicated in sporadic RCC, including *polybromo-1* (*PBRM1*), mutated in 37% of sporadic clear cell RCC (ccRCC).[8] *PBRM1* is located on 3p (as is the *VHL* gene), a region that is often deleted in ccRCC. PBRM1 forms part of the PBAF SWI/SNF chromatin remodeling complex that regulates gene transcription and DNA integrity. Genes associated with histone modifications have also been identified by large scale sequencing projects in ccRCC, although at a much lower frequency of mutations (1–4%). These include histone methylases (*SETD2* and *MLL2*) and histone demethylases (*JARID1C* and *UTX*).[9,10]

Epigenetic alterations play a significant role in the development and progression of human tumors. DNA methylation is a hallmark of many cancers and is increasingly utilized in clinical trials (epigenetic therapy) due to the reversible nature of the biological processes underlying DNA methylation. We and others identified *RASSF1A* tumor suppressor gene (TSG) to be frequently methylated in ccRCC as well as in other epithelial cancers, but to be rarely mutated in RCC and other cancers.[11,12] Hence, strategies to identify epigenetically inactivated genes in cancer can provide very useful molecular tools to understand the pathogenesis of cancer as well as to develop molecular markers for

*Correspondence to: Farida Latif; Email: f.latif@bham.ac.uk
Submitted: 12/10/12; Revised: 01/22/13; Accepted: 01/29/13
http://dx.doi.org/10.4161/epi.23817

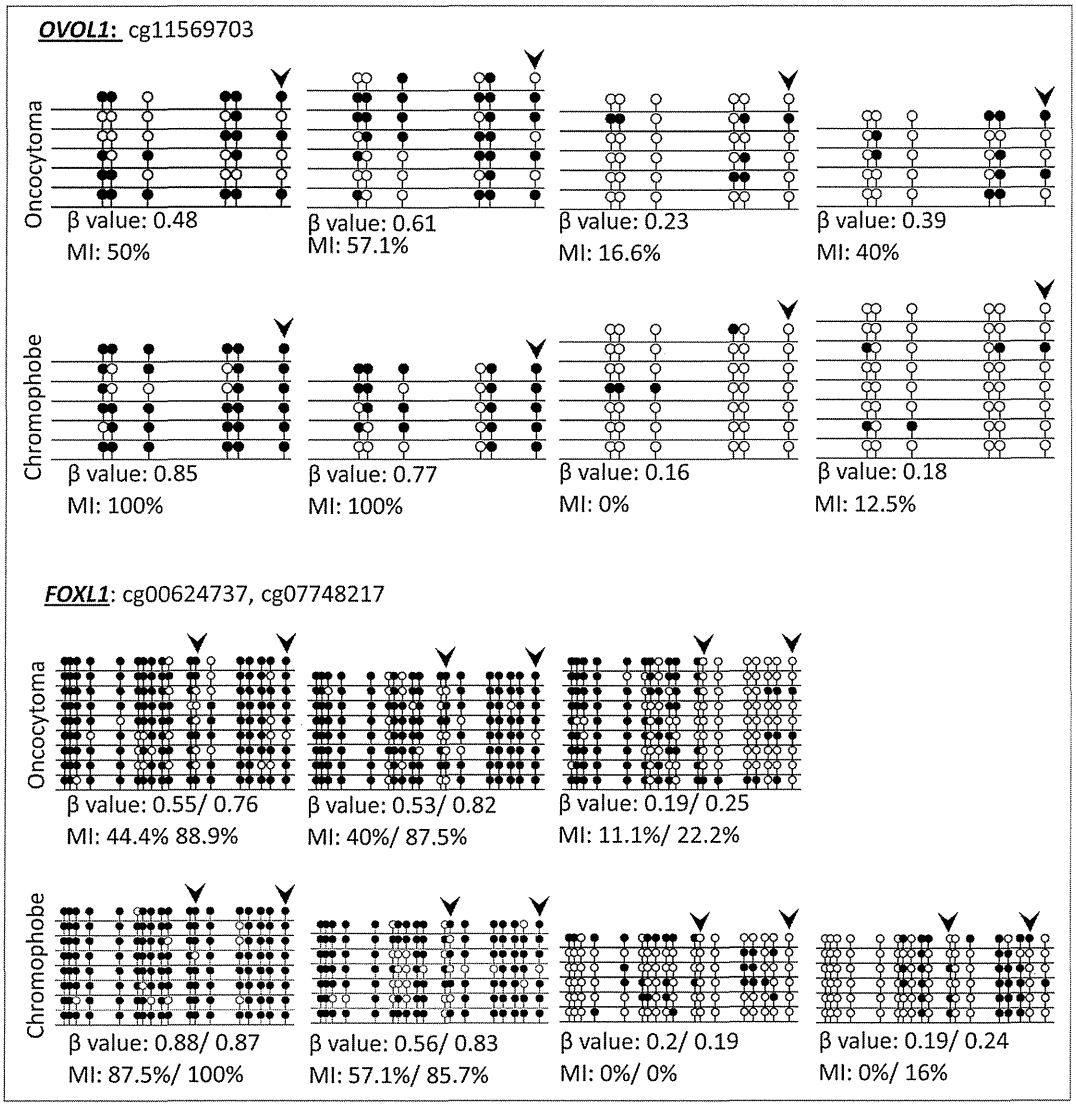


**Figure 1.** Validation of probe β values using bisulfite clone sequencing of *FOXL1* and *OVOL1*. Single colony sequencing of *FOXL1* and *OVOL1*, which were previously identified to be methylated in ccRCC and determined to be methylated with a β value > 0.5, was conducted in some of our samples. Hypermethylated loci (β value > 0.5) also showed a high methylation index (MI > 50%), while low β value loci correlated with a low MI. Bisulfite sequencing rows represent individual alleles, with each circle indicating location and methylation state of a CpG locus (black circle, methylated; white circle, unmethylated). Arrowheads indicate the HumanMethylation450 array locus under investigation. Also listed next to the gene name are the Target IDs.

diagnostic and prognostic purposes. In the past, we have used a range of molecular techniques, including candidate gene analysis and high throughput platforms such as MeDIP, functional epigenomics and genome-wide methylation arrays to elucidate the epigenome of ccRCC.[13-16] There is a dearth of knowledge in regards to epigenetic analysis of more rare types of RCC; hence, in the present report we have analyzed the epigenome of chromophobe RCC and renal oncocytomas using the latest Infinium HumanMethylation450 BeadChips to elucidate molecular pathways deregulated in these two entities and to help identify DNA methylation markers for the classification of renal tumors.

## Results

**Validation of the HumanMethylation450 BeadChips results.** Global methylation profiles of chromophobe RCC and renal oncocytoma samples in relation to four normal kidney samples were generated on the Infinium HumanMethylation450 BeadChips. A list of all probes methylated in > 30% of all the samples for each given RCC subtype is given in **Tables S1 and S2.**

The reproducibility of the HumanMethylation450 BeadChips results was examined via incorporation of a duplicate renal oncocytoma sample. Average β values for each locus were plotted to

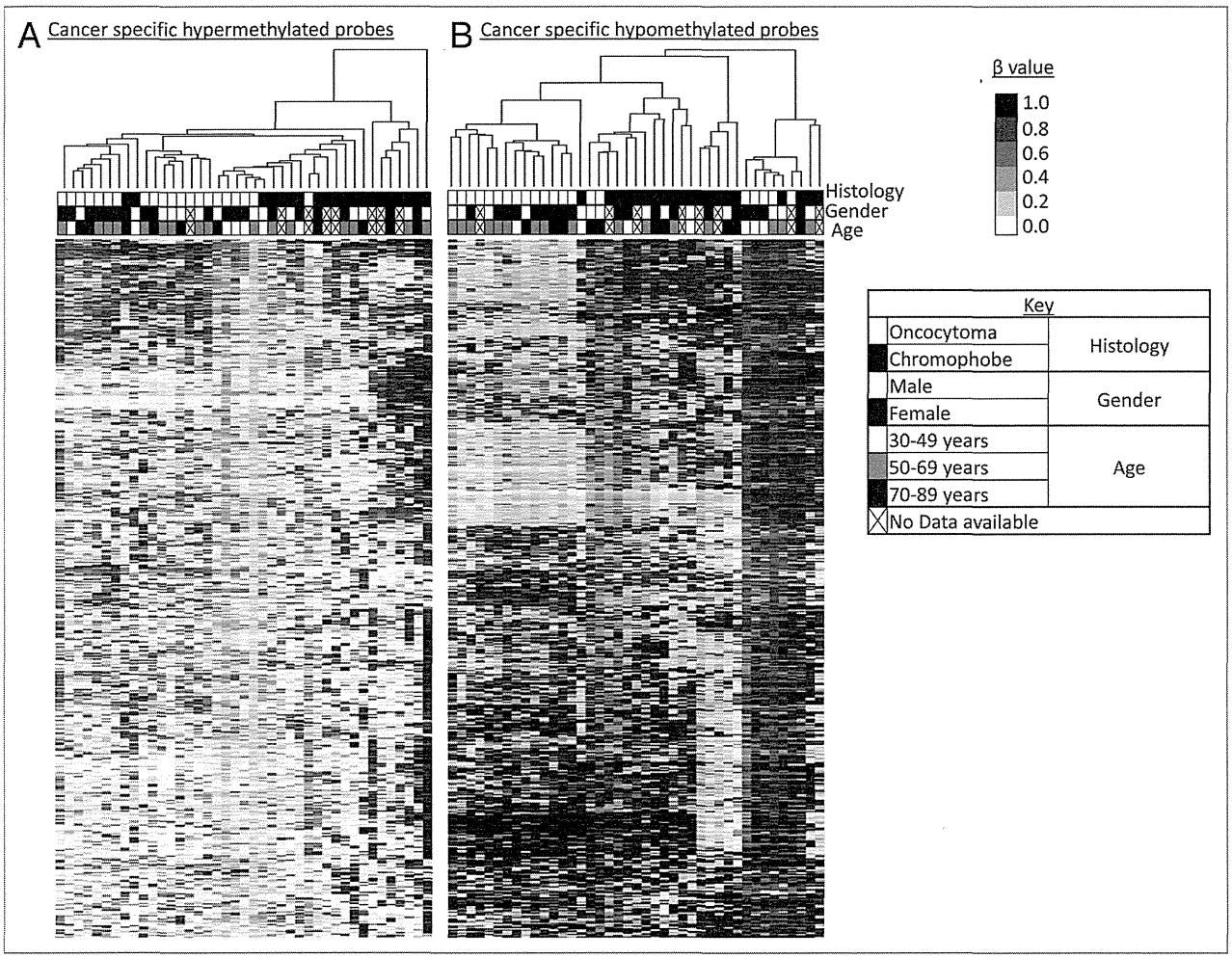


**Figure 2.** Supervised hierarchical clustering using Euclidean distance complete linkage of the 500 most variable cancer-specific hypermethylated (**A**) and hypomethylated (**B**) loci. Below the hierarchical cluster, the top row shows black squares for chromophobe samples and white squares for oncocytoma samples. Gender is denoted in the middle row: female by black squares and male by white squares. Patient age range is indicated in the lower row: 30–49 y, white squares; 50–69 y, gray squares; 70–89 y, black squares. Samples lacking these data are indicated by crossed out boxes. No clustering was observed in relation to gender or age.

identify correlation between the two replicates (**Fig. S1**). Pearson's correlation coefficient (r) was 0.997, indicating high correlation and, thus, reproducibility of the array.

Further confirmation of the HumanMethylation450 BeadChips results was obtained by single colony sequencing of bisulfite modified DNA of three genes (*BNC1*, *FOXL1* and *OVOL1*) previously identified to be frequently hypermethylated in ccRCC and also hypermethylated in our cohort.[16] Loci identified to be methylated (β value > 0.5) also showed a high methylation index (MI > 50%), while loci with low β values showed low MI (**Fig. 1**; **Fig. S2**).

**Chromophobe and oncocytoma methylome.** **Figure S3** depicts the stepwise analysis of the HumanMethylation450 data to identify cancer specific hyper- or hypo-methylation (see also Materials and Methods). We analyzed 20 chromophobe RCC samples and 21 renal oncocytoma samples as well as 4 normal kidney samples. For cancer specific hypermethylation, a CpG locus was considered hypermethylated if the β value was > 0.5 in the tumor sample (with all normal kidney samples showing a β value < 0.25) and hypomethylated if the β value was < 0.25 in the tumor sample (with all normal kidney samples showing a β value > 0.5).

Supervised hierarchical clustering using Euclidean distance complete linkage of the 500 most variable cancer specific hypermethylated loci identified two main clusters, with the majority of samples clustered in Cluster I and associated with a lower level of methylation (**Fig. 2A**). Sub-clustering within Cluster I reveals three further clusters with the trend to subdivide the samples according to histology. Cluster I.1 contained 7 oncocytoma samples and 2 chromophobe samples, Cluster I.2 contained 8 oncocytoma samples and Cluster I.3 possessed the majority of chromophobe samples within Cluster I (10) and only 6 oncocytoma samples. Cluster II contained 6 chromophobe samples with

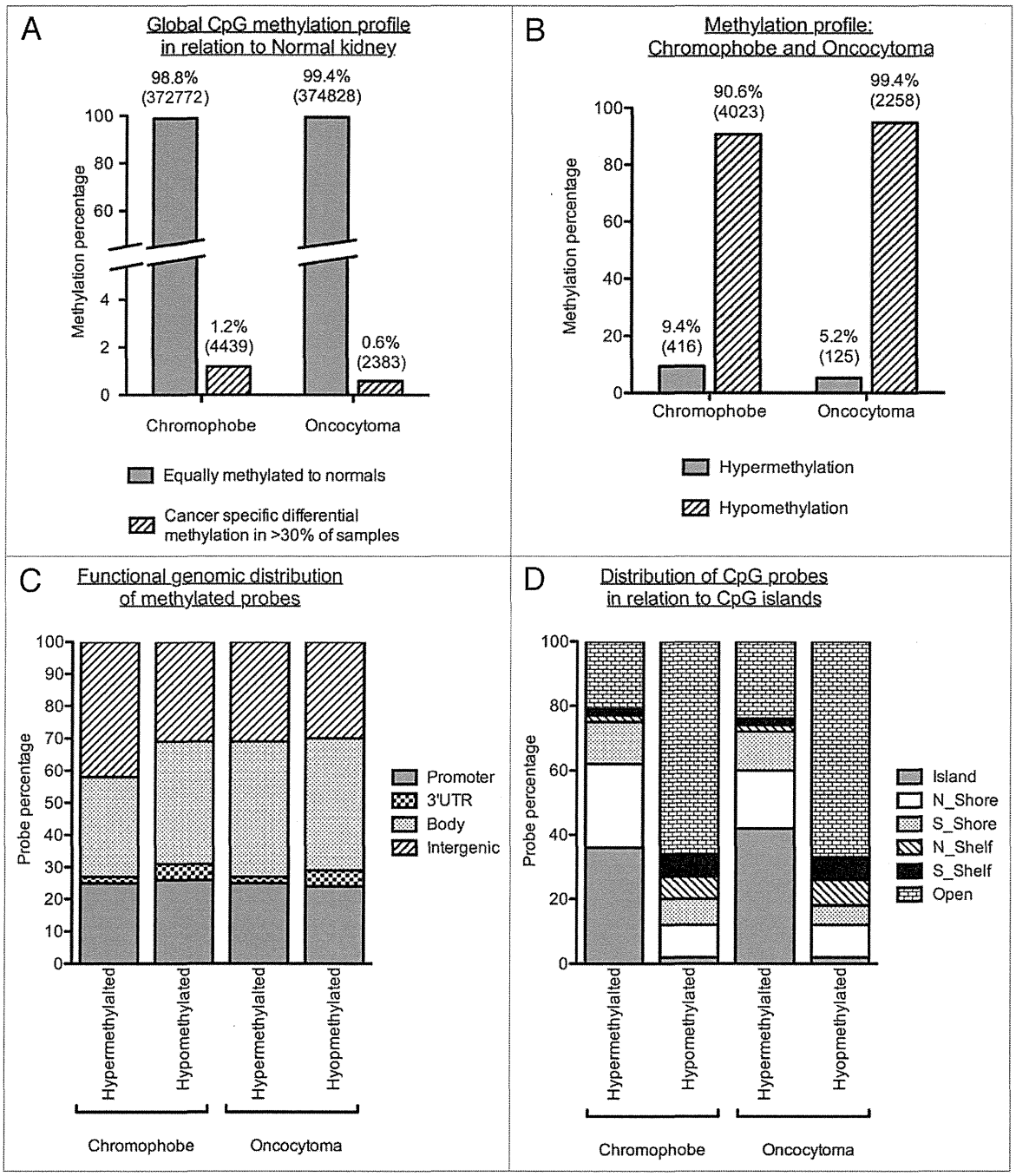


**Figure 3.** Methylation profiles of chromophobe RCC and renal oncocytoma samples. (**A**) Global methylation profile was mapped in relation to the 4 normal kidney samples included on the array. Differentially methylated loci were deemed to be all cancer-specific loci showing hyper- or hypo-methylation (1.2% or 4,439 loci for chromophobe samples and 0.6% or 2,383 loci for oncocytoma samples). All other loci not fulfilling this criterion where deemed to be equally methylated to the normal. (**B**) Methylation profile of cancer-specific loci identified as either hypermethylated (β value > 0.5) or hypomethylated (β value < 0.25) in > 30% of chromophobe RCC and > 30% renal oncocytoma samples. The majority of loci showed hypo-methylation in both histologies with less than 10% of cancer-specific probes being hypermethylated. (**C**) Genomic distribution of cancer-specific hyper- and hypo-methylated CpG loci in relation to their location within known genes. The promoter region indicates loci residing within the 1st exon, 5'UTR, TSS200 and TSS1500 of known genes. CpG distribution did not differ between the two histologies, or between the profiles of hypermethylated and hypomethylated loci. (**D**) Genomic distribution of cancer-specific hyper- and hypo-methylated CpG loci in relation to CpG density. The majority of hypermethylated loci are shown to reside in areas of high CpG density (CpG islands, north and south shores and north and south shelves): 79.1% for chromophobe samples and 76.0% for oncocytoma samples. Cancer-specific hypomethylated loci are mostly located in isolated/low-density CpG regions known as open sea (65.7% for chromophobe samples and 67.3% for oncocytoma samples).

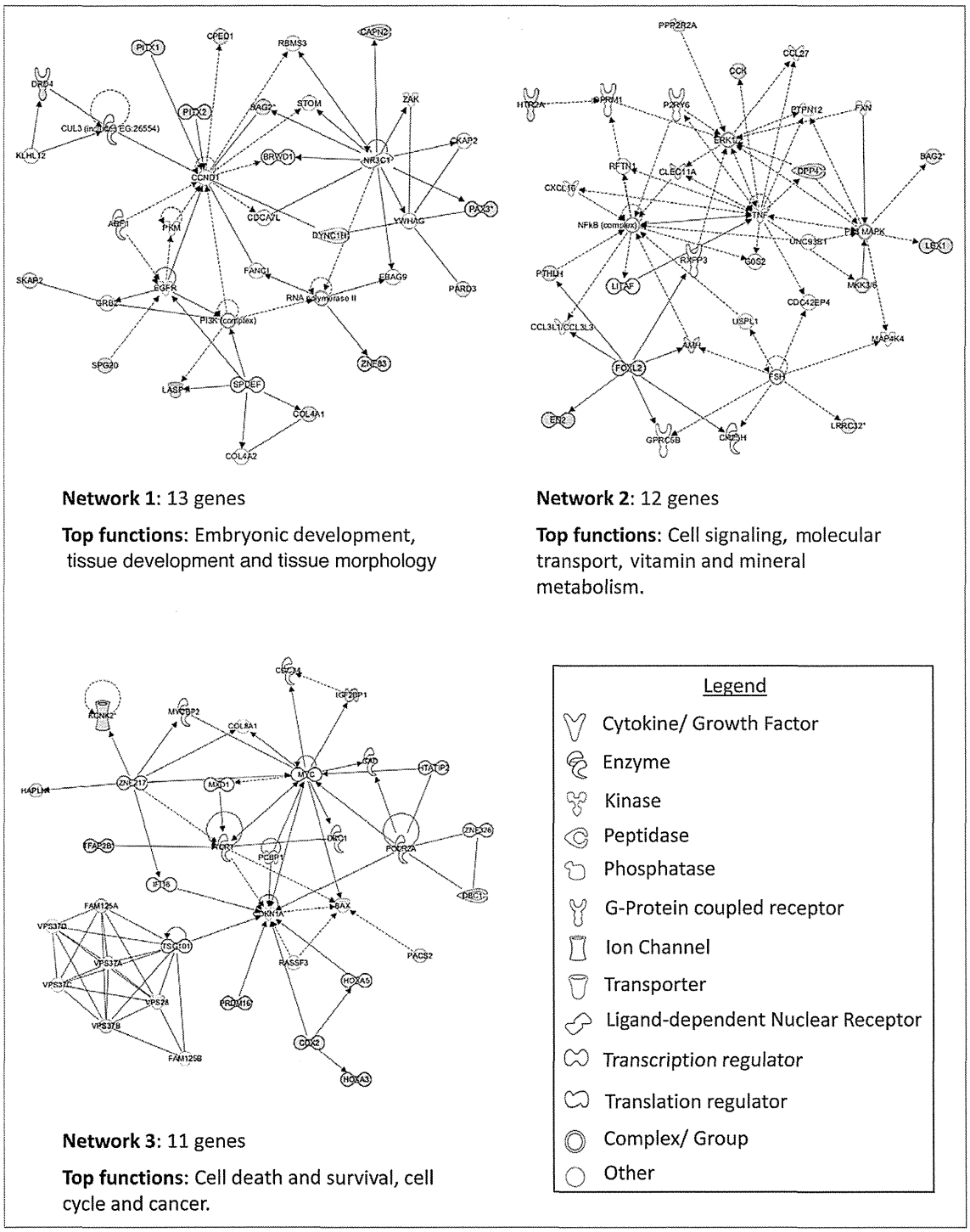


**Figure 4.** Top three networks identified by Ingenuity associated functional network analysis of genes hypermethylated in > 30% of chromophobe RCC samples. Methylated genes are shown in gray and connecting genes in white. Solid arrows represent direct interaction, dashed arrows highlight indirect interactions, solid joining lines identify protein binding only. IPA analysis identified several key networks with the top three showing interactions and involvement in embryonic development, tissue development and morphology, cell signaling, molecular transport, vitamin and mineral metabolism, cell death and survival, cell cycle and cancer.

the highest level of methylation and one chromophobe sample with widespread hypermethylation reminiscent of a CIMP positive phenotype (**Fig. 2A**). Supervised hierarchical clustering of the 500 most variable cancer specific hypomethylated loci also separated the two histologies, and grouped samples into four clusters. Cluster I presented the lowest levels of methylation and consisted predominantly of oncocytoma samples (14) and one chromophobe sample. Clusters II and III were composed predominantly of chromophobe samples (8 and 5, respectively), with only 2 oncocytoma samples, and presented an overall profile of methylation in the probes examined. Group IV clustered the samples with the lowest amount of hypomethylation and consisted of 5 oncocytoma samples and 4 chromophobe samples (**Fig. 2B**). No clustering was observed in relation to age or gender.

Global methylation profiling of chromophobe RCC and renal oncocytoma samples in relation to 4 normal kidney samples showed that only a small percentage of CpGs were differentially methylated between normal kidney and chromophobe RCC samples (1.2%) or oncocytoma RCC samples (0.6%) (**Fig. 3A**). Interestingly, both chromophobe RCC and renal oncocytoma samples presented a large proportion of loci that were hypomethylated (90.6% or 4,023 loci for chromophobe RCC and 99.4% or 2,258 loci for renal oncocytoma) with a smaller percentage of cancer-specific probes being hypermethylated in > 30% samples (chromophobe RCC: 9.4%, 416 loci, 204 genes; renal oncocytoma: 5.2%, 125 loci, 70 genes) (**Fig. 3B**; **Tables S1 and S2**). Investigation into the genomic distribution of the above hyper- and hypo-methylated loci in relation to known genes and CpG islands (CGIs) showed little variation between the two characterized cancers. It should also be noted that the percentage of loci residing in the promoter, 3'UTR, gene body or intergenic regions did not differ much between hyper- and hypo-methylated filters (**Fig. 3C**). The distribution of loci in relation to CGIs concurred with previous reports,[17] with a distinct trend showing that hypermethylation is mainly located in regions of dense CpG loci (CGI, shores and shelves), 79.1% and 76.0% for chromophobe RCC and renal oncocytoma samples, respectively. Hypomethylated loci were predominantly located in regions of low CpG density/isolated CpG loci, known as open sea (65.7% of chromophobe RCC samples and 67.3% of oncocytoma samples) (**Fig. 3D**).

**Hypermethylation profile analysis of chromophobe RCC and renal oncocytoma samples.** Within hypermethylated genes, only 17.5% (48 genes, 53 loci) were identified as methylated in both histologies. From literature searches, only a very small percentage of these genes (2.53% or 7 genes: *PCDH17, ASCL2, NKX6-2, HOXA9, PITX2, TLX3* and *ZNF177*) hypermethylated in either histology, had previously been reported as methylated in any type of renal cancer. Ingenuity pathway analysis (IPA) was conducted to identify interactions and networks among hypermethylated genes. The top three networks identified for genes methylated in > 30% of chromophobe samples included 13 genes associated with embryonic development, tissue development and tissue morphology, 12 genes associated with cell signaling, molecular transport and vitamin and mineral metabolism and 11 genes related to cell death and survival, cell cycle and cancer (**Fig. 4**). The top three networks for methylated genes in oncocytoma samples identified the following key functions: cell signaling and molecular transport (10 genes); cell morphology, cellular assembly and organization, cellular function and maintenance (10 genes) and cancer, cellular growth and proliferation and renal and urological disease (10 genes) (**Fig. 5**).

**Differentially hypermethylated loci between chromophobe RCC and renal oncocytoma samples.** A gene list of differentially hypermethylated loci between chromophobe RCC and renal oncocytoma samples was compiled by selecting CpG loci that were hypermethylated ($\beta$ value > 0.5) in > 30% of the samples of one tumor type and had a $\beta$ value < 0.3 in 90% of the samples of the other tumor. Student's t-test with FDR (false discovery rate)correction identified 30 genes (28 chromophobe-specific genes and 2 oncocytoma-specific genes) that showed significant differential methylation between the two types of RCC ($p < 0.05$) (**Table 1**). We confirmed the methylation status for two of the above genes (*NPHP4* and *SPG20*) by cloning and sequencing of bisulfite modified DNA (**Fig. 6**). All except one of the differentially methylated CpG loci resided in CGIs or shores, the remaining locus resided in a shelf. Twelve of the differentially hypermethylated CpG loci were associated with gene promoter CGIs or shores. DAVID and Panther analysis identified several genes to be involved in the Wnt signaling pathway (*EN2* and *HOXC4*), MAPK signaling pathway (*CACNG7*), Hippo pathway (*NPHP4*), TGF$\beta$ signaling pathway (*AMH*), cell death and apoptosis (*SPG20, NKX6-2, PAX3, BAG2*), as well as other functions such as cell cycle, cell migration and cell adhesion. Ingenuity pathway analysis (IPA) of the genes showing significant differential methylation identified several key networks with interactions in different pathways, including connective tissue development and function, embryonic and organ development, cancer, reproductive system disease and cellular development (**Fig. 7**).

To further investigate chromophobe-specific hypermethylation, the 28 genes differentially methylated in chromophobe RCC samples vs. renal oncocytoma samples were compared with The Cancer Genome Atlas (TCGA) data for ccRCC (n = 100) and papillary renal cell carcinoma (n = 81). One-way ANOVA with Games-Howell post hoc test for unequal sample sizes identified significant chromophobe-specific hypermethylation in three genes: *SPG20*, *NPHP4* and *TFAP2B* (**Fig. 8A**).

The same criterion was applied to investigate oncocytoma-specific hypermethylation in two differentially methylated loci. Post hoc analysis identified one locus (*ALCAM*) to be differentially hypermethylated in oncocytoma samples. Interestingly, the other gene, *HOXA9*, which was initially included due to being significantly methylated in chromophobe samples, has been identified instead as being unmethylated in oncocytoma, while showing significantly higher levels of methylation in all other histologies of renal carcinoma (**Fig. 8B**).

**Hypomethylation profile analysis of chromophobe RCC and renal oncocytoma samples.** Profiling was then conducted on gene-associated loci identified as hypomethylated in > 30% chromophobe and oncocytoma samples. A total of 2,134 genes (4,023 loci) and 1,239 genes (2,258 loci) were identified to be hypomethylated in chromophobe and oncocytoma samples, respectively. Of these genes, 27.9% (943 genes, 1,543 loci) were identified to be

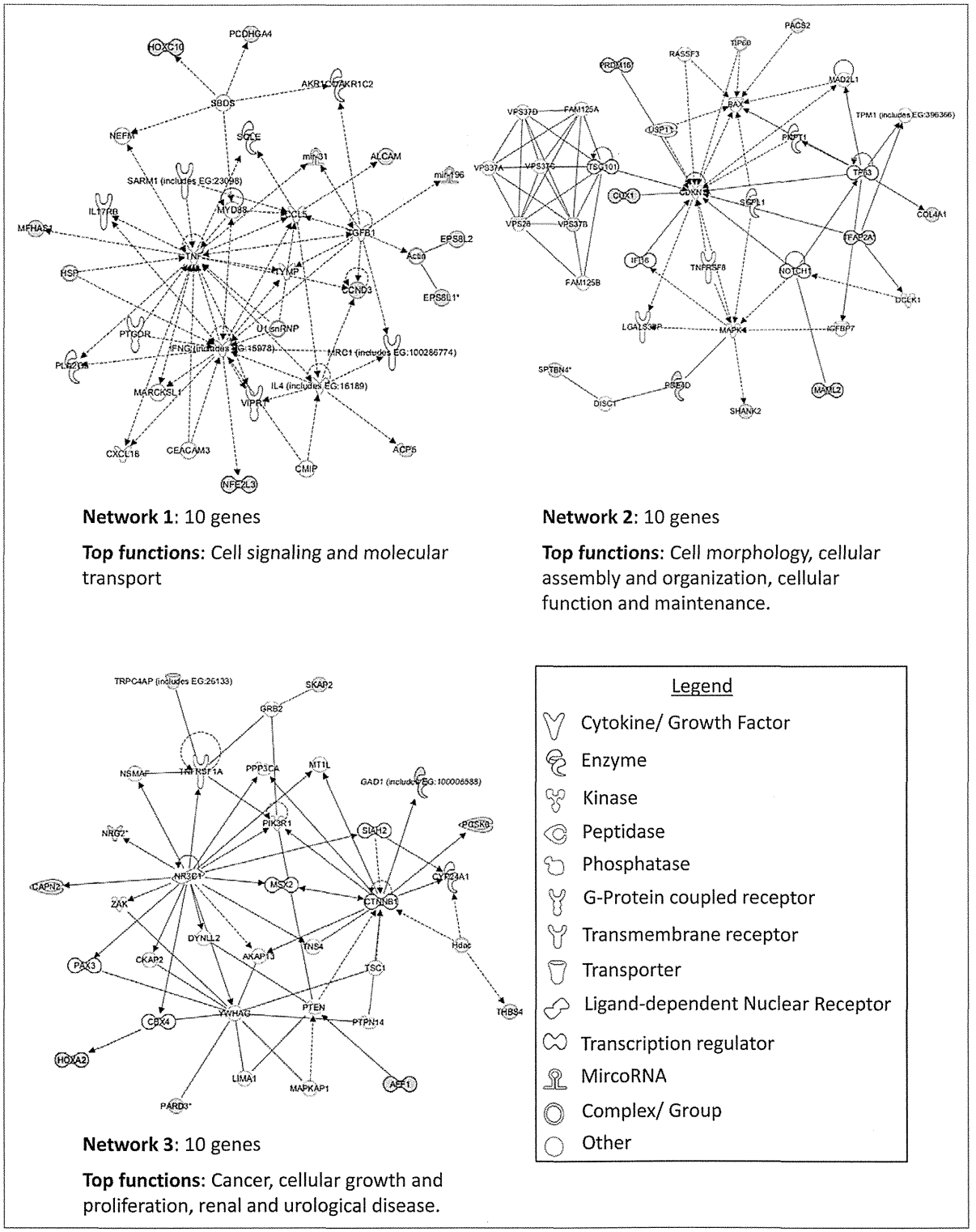


**Network 1**: 10 genes

**Top functions**: Cell signaling and molecular transport

**Network 2**: 10 genes

**Top functions**: Cell morphology, cellular assembly and organization, cellular function and maintenance.

**Network 3**: 10 genes

**Top functions**: Cancer, cellular growth and proliferation, renal and urological disease.

**Figure 5.** Top three networks identified by Ingenuity associated functional network analysis of genes hypermethylated in > 30% of renal oncocytoma samples. Methylated genes are shown in gray and connecting genes are in white. Solid arrows represent direct interaction, dashed arrows highlight indirect interactions, solid joining lines identify protein binding only. IPA analysis identified networks with involvement in cell signaling and molecular transport, cell morphology, cellular assembly and organization, cellular function and maintenance, cancer, cellular growth and proliferation, and renal and urological disease.

**Table 1.** Differentially hypermethylated genes between chromophobe RCC and renal oncocytoma samples

| Gene symbol | Cancer | Target ID | Relation to gene | CpG region | Meth in Onco (β value > 0.5) | Meth in Chromo (β value > 0.5) | Normal kidney | Corrected p Value | Chr |
|---|---|---|---|---|---|---|---|---|---|
| ALCAM | Oc | cg05645404 | Body | N_Shore | 12/21 (57.1%) | 0/20 (0.0%) | 0/4 | 4.20E-05 | 3 |
| TFAP2B | Ch | cg05437823 | 3'UTR | Island | 0/21 (0.0%) | 8/20 (40.0%) | 0/4 | 0.0019 | 6 |
| TRPC4AP; TRPC4AP | Oc | cg01154966 | TSS1500; TSS1500 | Island | 7/21 (33.3%) | 0/20 (0.0%) | 0/4 | 0.0034 | 20 |
| HOXA9 | Ch | cg03217995 | Body | N_Shore | 0/21 (0.0%) | 8/20 (40.0%) | 0/4 | 0.0036 | 7 |
| DBC1 | Ch | cg03625109 | TSS1500 | Island | 0/21 (0.0%) | 7/20 (35.0%) | 0/4 | 0.0038 | 9 |
| CACNG7 | Ch | cg21477176 | 3'UTR | S_Shore | 1/21 (4.8%) | 6/20 (30.%) | 0/4 | 0.0043 | 19 |
| NKX6–2 | Ch | cg11174855 | 3'UTR | Island | 1/21 (4.8%) | 7/20 (35.0%) | 0/4 | 0.0043 | 10 |
| NPHP4 | Ch | cg20383686 | TSS200 | Island | 0/21 (0.0%) | 6/20 (30.%) | 0/4 | 0.0048 | 1 |
| AMH | Ch | cg05345154 | Body | Island | 0/21 (0.0%) | 6/20 (30.%) | 0/4 | 0.0065 | 19 |
| DPP4 | Ch | cg19350270 | Body | N_Shore | 0/21 (0.0%) | 7/20 (35.0%) | 0/4 | 0.0066 | 2 |
| SOX2OT | Ch | cg24513480 | Body | N_Shelf | 1/21 (4.8%) | 8/20 (40.0%) | 0/4 | 0.0072 | 3 |
| EN2 | Ch | cg12034383 | TSS1500 | Island | 0/21 (0.0%) | 6/20 (30.%) | 0/4 | 0.0073 | 7 |
| SPG20; SPG20; SPG20; SPG20 | Ch | cg10558887 | 5'UTR; 5'UTR; 5'UTR; 5'UTR | N_Shore | 0/21 (0.0%) | 7/20 (35.0%) | 0/4 | 0.0075 | 13 |
| RALYL; RALYL; RALYL; RALYL; RALYL | Ch | cg22403811 | 5'UTR; TSS1500; 5'UTR; 5'UTR; 1stExon | N_Shore | 0/21 (0.0%) | 6/20 (30.%) | 0/4 | 0.0096 | 8 |
| JSRP1 | Ch | cg04887494 | Body | Island | 0/21 (0.0%) | 6/20 (30.%) | 0/4 | 0.0098 | 19 |
| PAX3; PAX3; PAX3; PAX3; PAX3; PAX3; PAX3; PAX3; CCDC140 | Ch | cg13767755 | Body; Body; Body; Body; Body; Body; Body; Body; TSS200 | N_Shore | 0/21 (0.0%) | 6/20 (30.%) | 0/4 | 0.0184 | 2 |
| PITX1 | Ch | cg00396667 | 3'UTR | Island | 1/21 (4.8%) | 6/20 (30.%) | 0/4 | 0.0188 | 5 |
| SH3PXD2A | Ch | cg18735015 | Body | Island | 1/21 (4.8%) | 6/20 (30.%) | 0/4 | 0.0213 | 10 |
| SIX2 | Ch | cg24887265 | Body | N_Shore | 0/21 (0.0%) | 6/20 (30.%) | 0/4 | 0.0219 | 2 |
| TOX2; TOX2; TOX2 | Ch | cg10900455 | 5'UTR; Body; 5'UTR | Island | 1/21 (4.8%) | 6/20 (30.%) | 0/4 | 0.0224 | 20 |
| HAPLN1 | Ch | cg12199221 | TSS200 | N_Shore | 0/21 (0.0%) | 6/20 (30.%) | 0/4 | 0.0226 | 5 |
| IRX6 | Ch | cg01064265 | Body | Island | 1/21 (4.8%) | 7/20 (35.0%) | 0/4 | 0.0230 | 16 |
| NKAPL | Ch | cg17384889 | TSS200 | Island | 0/21 (0.0%) | 6/20 (30.%) | 0/4 | 0.0236 | 6 |
| LBX1 | Ch | cg03053579 | Body | Island | 0/21 (0.0%) | 6/20 (30.%) | 0/4 | 0.0237 | 10 |
| BAG2 | Ch | cg10230427 | Body | S_Shore | 1/21 (4.8%) | 7/20 (35.0%) | 0/4 | 0.0242 | 6 |
| MKX | Ch | cg26298409 | Body | Island | 0/21 (0.0%) | 6/20 (30.%) | 0/4 | 0.0262 | 10 |
| SLITRK1 | Ch | cg16727923 | 1stExon | Island | 1/21 (4.8%) | 7/20 (35.0%) | 0/4 | 0.0376 | 13 |
| BAG2 | Ch | cg27164797 | Body | S_Shore | 0/21 (0.0%) | 6/20 (30.%) | 0/4 | 0.0401 | 6 |
| KRT27 | Ch | cg02399249 | Body | Island | 0/21 (0.0%) | 6/20 (30.%) | 0/4 | 0.0421 | 17 |
| HHEX | Ch | cg09721427 | TSS1500 | Island | 0/21 (0.0%) | 6/20 (30.%) | 0/4 | 0.0476 | 10 |

Oc, renal oncocytoma; Ch, chromophobe RCC; Chr, chromosome.

hypomethylated in both histologies. IPA analysis for each histology identified association with many networks, with the top three networks for each histology displayed in **Figures S4 and S5**. The top three networks identified by IPA for chromophobe have functions involved in cell to cell signaling, hereditary disorders, neurological diseases, post-translational modifications, tissue morphology, cancer and gastrointestinal diseases (**Fig. S4**). On the other hand, the top three IPA networks for oncocytoma have been associated with functions in hereditary disorder, neurological disease, skeletal and muscular disorders, cancer, cellular development, cellular function and maintenance, embryonic development, lymphoid tissue structure and development, and organ development (**Fig. S5**).

**Differentially hypermethylated loci between chromophobe RCC and renal oncocytoma samples.** Differentially hypomethylated genes between chromophobe and oncocytoma samples were identified as having a β value < 0.25 in > 30% of the samples in one histology and a β value > 0.45 in 100% of the samples of the other histology. Student's t-test with FDR correction identified 43 loci (41 genes: 5 genes in oncocytoma and 36 genes in chromophobe samples) differentially hypomethylated (**Table 2**). Further IPA analysis of the genes showing significant differential hypomethylation between chromophobe RCC and renal oncocytoma samples identified associations with several functions, including cardiovascular system development and function, cell cycle, cell death and survival, cellular development, skeletal and muscular system development and function, and cellular growth and proliferation (**Fig. 9**).

## Discussion

Chromophobe RCC and renal oncocytoma are thought to arise from distal renal tubules. Chromophobe RCCs have better prognosis than ccRCC or papillary RCC, with fewer than 5% of the cases being metastatic at the time of diagnosis, while renal oncocytomas are benign tumors morphologically similar to chromophobe RCC.[1] Hence, differential diagnosis of these two types of renal tumors is of paramount importance in determining the clinical course of treatment. Chromosomal abnormalities, gene expression and miRNA profiles have been used to try to distinguish between renal oncocytomas and chromophobe RCCs. Renal oncocytomas, as expected of a benign tumor, show a limited number of chromosomal abnormalities, including loss of chromosomes 1 and Y. On the other hand, frequent losses of chromosomes 1, 2, 6, 10 and 17 have been identified in chromophobe RCC. Loss of chromosomes 2, 10, 13, 17 and 21 are also reported to discriminate between chromophobe RCC and renal oncocytomas.[18] Using a combination of gene expression and high throughput SNP platforms, Tan et al. generated a probe signature that could discriminate chromophobe RCC and renal oncocytomas.[19] Petillo et al. identified a unique miRNA signature for clear cell, papillary, chromophobe RCC and renal oncocytoma.[20]

There is growing evidence that not only genetic but also epigenetic changes play important roles in human malignancy. Aberrant DNA methylation leading to alterations in normal gene regulation was one of the first epigenetic marks to be associated with cancer development and has been recognized for over 20 years. DNA hypomethylation associated with loss of DNA methylation occurs in many gene poor regions, including introns, repetitive sequences and retrotransposons, and results in chromosomal instability. DNA hypermethylation associated with gain of methylation in promoter CGIs silences tumor suppressor genes. A more recent study has identified that the majority of DNA methylation changes involved in regulation of gene expression are located at CpG shores, located up to 2 kb distant from CGIs.[21]

Previously, our laboratory and others have used the Illumina Goldengate methylation BeadChips (containing 1,505 CpG sites in 807 genes) to identify methylated TSGs in RCC.[22] More recently, we have identified novel methylated TSGs in RCC by using the much more comprehensive Illumina HumanMethylation27 BeadChips, which interrogate approximately 27,500 CpG in > 14,000 genes.[16] The above studies analyzed the more frequently occurring histological RCCs, namely ccRCC and papillary RCC, while there is very little knowledge regarding the epigenome of less frequently occurring histological subtypes of RCC. Hence, we have used the most comprehensive high density HumanMethylation450 BeadChips (> 480,000 CpG dinucleotides in > 20,600 genes) to elucidate the epigenome of the more rare and less malignant types of RCC, namely chromophobe RCC and renal oncocytomas. Our previous analysis using the Goldengate methylation arrays showed that papillary RCC had much higher numbers of methylated loci compared with ccRCC, irrespective of the VHL status of the ccRCC.[22] In the present study, we demonstrate that malignant chromophobe RCCs show higher percentage of cancer-specific hypermethylated loci, compared with the benign renal oncocytomas, although both entities demonstrate a much larger number of hypomethylated loci compared with hypermethylated loci. Only a minority of the genes frequently hypermethylated in chromophobe RCC and renal oncocytoma samples have been previously shown to be frequently methylated in RCC (< 3%).

Among the 30 CpG loci showing significant differential hypermethylation between chromophobe RCC and renal oncocytoma samples, 12 CpG loci were associated with gene promoter CGIs or shores, hence likely to influence gene regulation (11 in chromophobe RCC and 1 in renal oncocytoma samples). Furthermore, 5 of the 11 differentially hypermethylated loci associated with gene promoter CGIs or shores in RCC reside on chromosomes that are frequently lost from the genomes of ccRCC and are associated with downregulation of gene expression,[18] constituting classical hallmarks of TSG loci. Functional pathway analysis showed that, among the differentially methylated genes, some were involved in key signaling pathways, including Wnt, MAPK, TGFβ, Hippo pathway and cell death and apoptosis. While 71% of differentially hypomethylated loci between chromophobe RCC and renal oncocytoma samples resided in isolated CpGs (open sea), 10 of the 37 differentially hypomethylated loci in chromophobe RCC resided on chromosomes that showed chromosomal gains in this tumor type.

In addition, we utilized TCGA data on ccRCC and papillary RCC to determine if any of the differentially hypermethylated genes remained significant when considering all four types of histological RCC. This analysis yielded three genes (*SPG20, NPHP4* and *TFAP2B*) that remained differentially hypermethylated in chromophobe RCC compared with ccRCC, papillary RCC and renal oncocytoma. Similar analysis yielded one gene (*ALCAM*) that showed differential hypermethylation in renal oncocytoma when comparing the four histological subtypes of RCC. The differentially methylated CpG loci in *NPHP4* and *SPG20* resided in gene promoter CGIs and shores, respectively. *SPG20* promoter hypermethylation has recently been described as a biomarker for early detection of colorectal cancer and plays a role in cytokinesis arrest in cancer cells.[23] *NPHP4* is a cilia-associated protein involved in Wnt and Hippo tumor suppressor networks.[24]

The differentially methylated genes we have identified may provide clues into the biological differences among the RCC subtypes